ELSEVIER

Inorganica Chimica Acta 271 (1998) 160–166

Inorganica Chimica Acta

Comparative time-resolved IR and UV spectroscopic study of monophosphine and diphosphine platinum(II) azido complexes

Horst Hennig [a,*], Klaus Ritter [a], Alexander K. Chibisov [b,1], Helmut Görner [b], Friedrich-Wilhelm Grevels [b], Klaus Kerpen [b], Kurt Schaffner [b]

[a] *Universität Leipzig, Institut für Anorganische Chemie, Talstraße 35, D-04103 Leipzig, Germany*

[b] *Max-Planck-Institut für Strahlenchemie, D-45413 Mülheim an der Ruhr, Germany*

Received 23 May 1997; revised 10 July 1997; accepted 31 July 1997

Abstract

Solutions of *cis*-diazido-bis(triphenylphosphine)platinum(II) (*cis*-$[Pt^{II}(PPh_3)_2(N_3)_2]$) and diazido-1,3-bis(diphenylphosphino)-propaneplatinum(II) ($[Pt^{II}(dppp)(N_3)_2]$) were studied by time-resolved IR and UV–Vis absorption spectroscopy after excitation by 308 nm laser pulses. Photoinduced electron transfer reduces $[Pt^{II}(dppp)(N_3)_2]$ to $[Pt^{I}(dppp)N_3]$ (IR maximum 2045 cm^{-1}) which decays in several solvents at room temperature (half-life ~0.3 ms) via intramolecular electron transfer to coordinatively unsaturated $[Pt^{0}(dppp)]$. With *cis*-$[Pt^{II}(PPh_3)_2(N_3)_2]$, photoisomerization to *trans*-$[Pt^{II}(PPh_3)_2(N_3)_2]$ (IR maximum 2050 cm^{-1}) and photoreduction compete as primary photoreactions, whereas the decay of $[Pt^{I}(PPh_3)_2N_3]$ is analogous to that of $[Pt^{I}(dppp)N_3]$. Oxygen scavenges $[Pt^{I}(PPh_3)_2N_3]$ and $[Pt^{I}(dppp)N_3]$ with rate constants $k_{ox} = (1.3–2.8) \times 10^7$ M^{-1} s^{-1}. The photochemistry of *cis*-$[Pt^{II}(PPh_3)_2(N_3)_2]$ and $[Pt^{II}(dppp)(N_3)_2]$ in the absence and presence of O_2 is discussed. © 1998 Elsevier Science S.A.

Keywords: Platinum complexes; Azido complexes; Electron transfer

1. Introduction

Mixed-ligand transition metal azido complexes distinguish themselves by a large variety of photochemical reaction pathways. Photoinduced substitution, isomerization and redox reactions can take place depending on the nature of the central ion, the wavelength of irradiation and the solvent used [1]. The central ion strongly influences the path of intramolecular electron transfer reactions when azide ligands are participating. The formation of azidyl radicals ($^{\bullet}N_3$) [2] and nitrene intermediates [3,4] has been described along with the generation of nitrido complexes [5]. However, the mechanism of photoinduced electron transfer reactions, where azide ligands are involved, has received little attention [1,6–9]. No theoretical approach, except for Basolo's rather tentative rule [10], exists which allows a prediction of the redox properties of metal azido complexes. Clearly, further investigation of various kinds of transition metal azido complexes is required to gain a satisfactory insight into their photochemical behaviour.

In completing our earlier results [6–9], this paper deals with further experimental findings concerning the primary photoreaction of *cis*-diazido-bis(triphenylphosphine)platinum(II) (*cis*-$[Pt^{II}(PPh_3)_2(N_3)_2]$, PPh_3 = triphenylphosphine) in comparison with diazido-1,3-bis(diphenylphosphino)-propaneplatinum(II) ($[Pt^{II}(dppp)(N_3)_2]$, dppp = 1,3-bis-(diphenylphosphino)propane), where the bidentately coordinated diphos ligand dppp prevents *cis* → *trans* isomerization. Because the IR absorption of these two complexes in the 2100–2000 cm^{-1} range is very sensitive to changes within their first coordination sphere, time-resolved IR absorption spectroscopy was used to distinguish between intramolecular electron transfer and *cis* → *trans* photoisomerization. So far as we know, these are the first results in the detection of photochemically generated intermediates based on Werner-type complexes by means of time-resolved IR spectroscopy.

2. Experimental

cis-$[Pt^{II}(PPh_3)_2(N_3)_2]$ and $[Pt^{II}(dppp)(N_3)_2]$ were synthesized according to the literature [12]. 2-Methyltetra-

* Corresponding author: Tel.: +49 341 973 6150; fax: +49 341 960 4600; e-mail: hennigho@sonne.tachemie.uni-leipzig.de

[1] Permanent address: N.N. Semenov Institute of Chemical Physics, Russian Academy of Sciences, 117421 Moscow, Russia.

PII S0020-1693(97)05947-1

hydrofuran (MeTHF) was purified by distillation. The other solvents (Merck) were used as commercially available.

The ground state absorption data of *cis*-[Pt(PPh$_3$)$_2$(N$_3$)$_2$] in CH$_3$CN are $\lambda_{max}=267$ nm, $\varepsilon_{267}=2.4\times10^4$ M^{-1} cm^{-1} ($\varepsilon_{308}=4.5\times10^3$ M^{-1} cm^{-1}) and $\varepsilon=4\times10^3$ M^{-1} cm^{-1} at 2060 cm^{-1}. Those of [Pt(dppp)(N$_3$)$_2$] are $\lambda_{max}=265$ nm, $\varepsilon_{265}=2.2\times10^4$ M^{-1} cm^{-1} ($\varepsilon_{308}=1.6\times10^3$ M^{-1} cm^{-1}) and $\varepsilon=3\times10^3$ M^{-1} cm^{-1} at 2060 cm^{-1}. The values in CH$_2$Cl$_2$ are $\varepsilon_{308}=5.8\times10^3$ and 2.2×10^3 M^{-1} cm^{-1} for *cis*-[Pt(PPh$_3$)$_2$(N$_3$)$_2$] and [Pt(dppp)(N$_3$)$_2$] respectively.

An XeCl excimer laser (Lambda Physik, EMG 200), with a pulse width of 20 ns and a maximum energy of 0.2 J, was used for excitation at 308 nm. Time-resolved UV–Vis and IR transient absorption spectra were obtained by means of laser flash photolysis. For IR detection (rise time ~2 μs, 1 mm CaF$_2$ cell) essentially the same set-up was used as described previously [13]. The laser beam was lightly focused by a cylindrical quartz lens (focal length 30 cm), which took into account the rather large divergence. The excitation intensity, which was reduced by wire-mesh filters, was limited to ~30 MW cm^{-2} because of shock waves at higher intensities under our conditions. The absorbances where kept to $A_{308}=0.2$–0.6 (path length 1 mm), corresponding to concentrations of 0.2–0.6 mM and 1–4 mM for *cis*-[Pt(PPh$_3$)$_2$(N$_3$)$_2$] and [Pt(dppp)(N$_3$)$_2$] respectively. The samples were saturated by purging with Ar (20–30 min), air or O$_2$, and fresh solutions were used for each flash via a flow through system. For UV–Vis detection (rise time 10 ns, 1 cm quartz cell) two transient digitizers (Tektronix 7912AD and 390AD) and a computer (Archimedes 440) were used [14]. The laser beam was focused by a spherical and a cylindrical quartz lens (focal lengths 1 m and 10 cm respectively). The (first) half-life ($t_{1/2}$) and the lifetime (τ) in the absence or presence of O$_2$, respectively, refer to the changes after the pulse and the quasi-constant absorption changes after appropriate times. It should be noted that too high a dose of the analysing light beam leads to an increase in ΔA_{380} in the 0.01–1 s time range. Such an artifact may account for the previously reported increase in ΔA in the 320–450 nm range between 0.01–0.9 s for *cis*-[Pt(PPh$_3$)$_2$(N$_3$)$_2$] in CH$_3$CN [6]. All measurements were carried out in solution at 23 ± 2°C.

3. Results and discussion

3.1. Time-resolved IR absorption spectroscopy ([Pt(dppp)(N$_3$)$_2$])

The transient IR difference spectrum of [Pt(dppp)(N$_3$)$_2$] in Ar-saturated CH$_2$Cl$_2$ solution shows strong bleaching in the 2080–2050 cm^{-1} range within 2–3 μs after the exciting 308 nm pulse. The maximum at 2064 cm^{-1} and a weak absorption around 2040 cm^{-1} disappear within several milliseconds (Fig. 1). The bleaching is attributed to photodecomposition, rather than to an observable intermediate, in view of the fact that the spectra of the transient difference at

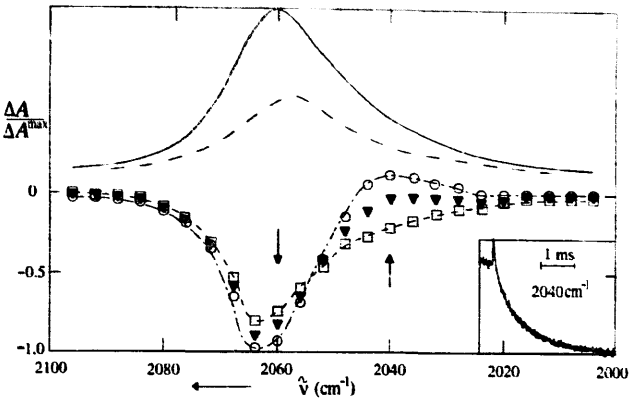

Fig. 1. Transient difference IR spectra ($\Delta A^{max}\sim-0.06$) of [Pt(dppp)(N$_3$)$_2$] in Ar-saturated CH$_2$Cl$_2$ at 0.005 ms (○), 0.3 ms (▼) and 2 ms (□) after the 308 nm pulse. Inset: kinetics at 2040 cm^{-1}. The upper curves refer the ground state spectrum prior to and after ~30 pulses (full and dashed lines respectively).

1–10 ms and of the ground state are practically identical, i.e. the stable photoproducts do not absorb in the 2100–2000 cm^{-1} range.

The kinetics in the bleaching and absorption area are essentially the same within experimental error. They follow a mixed first- and second-order law at higher excitation intensity (>10 MW cm^{-2}) and essentially a first-order law at lower intensity (<5 MW cm^{-2}), the rate constant being $\sim2\times10^3$ s^{-1}. These observations reflect the existence of two species, one IR-absorbing intermediate after the pulse I_A ([Pt^I(dppp)N$_3$]) and a second intermediate I_B not absorbing in the IR region monitored (I_B [Pt^0(dppp)]; bleaching of the IR ground state spectrum). I_A and I_B are formed consecutively:

$$[Pt(dppp)(N_3)_2] \xrightarrow{h\nu} I_A([Pt^I(dppp)N_3]) \rightarrow I_B([Pt^0(dppp)]) \quad (1)$$

Similar results and a half-life of $t_{1/2}\approx0.3$ ms were obtained for [Pt(dppp)(N$_3$)$_2$] in Ar-saturated CH$_3$CN solutions. The spectral changes are similar in air-saturated CH$_3$CN, while both the decay of the initial transient and the formation of the second bleaching component are faster. From the half-life under Ar and the lifetimes in air- and O$_2$-saturated CH$_3$CN (Table 1), a rate constant for scavenging by O$_2$ of $k_{ox}\approx1.5\times10^7$ M^{-1} s^{-1} was obtained. From these results we conclude that the reaction of I_A with O$_2$ leads to a species which, like [Pt^0(dppp)], has no absorption in the IR region monitored. In tetrahydrofuran (THF) and CHCl$_3$ the spectra are similar, and in all four solvents a trend to shorter $t_{1/2}$ values was found on going from Ar- to air- and O$_2$-saturated solution.

3.2. Time-resolved IR absorption spectroscopy (*cis*-[Pt(PPh$_3$)$_2$(N$_3$)$_2$])

The transient difference spectrum of *cis*-[Pt(PPh$_3$)$_2$(N$_3$)$_2$] in Ar-saturated CH$_2$Cl$_2$ within 2–3 μs after the pulse

Table 1
Half-lives under Ar and lifetimes in the presence of O_2, obtained from IR measurements [a]

Compound	Solvent	$t_{1/2}$ [b] (μs) Ar	τ (μs) air
[Pt(dppp)$(N_3)_2$]	THF	300	21
	$CHCl_3$	250	28
	CH_2Cl_2	330	42
	CH_3CN	300	35
cis-[Pt$(PPh_3)_2(N_3)_2$]	THF	300	22
	$CHCl_3$	250	<40
	CH_2Cl_2	290	43
	CH_3CN	300	35

[a] A_{308} = 0.2–0.6 (1 mm), λ_{exc} = 308 nm; the solutions were purged with Ar or air; the lifetimes in O_2-saturated solutions are generally ≤ 10 μs.
[b] Note that the excitation intensity was kept constant.

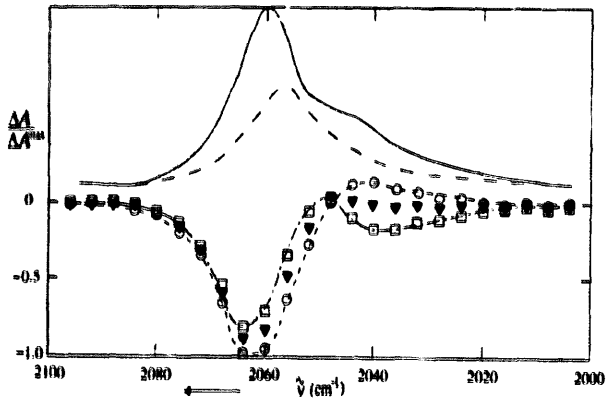

Fig. 2. Transient difference IR spectra ($\Delta A^{max} \approx -0.06$) of *cis*-[Pt$(PPh_3)_2(N_3)_2$] in Ar-saturated CH_2Cl_2 at 0.005 ms (○), 0.3 ms (▼) and 2 ms (□) after the 308 nm pulse. The upper curves refer to the ground state spectrum prior to and after ≈ 30 pulses (full and dashed lines respectively).

shows strong bleaching in the range 2080–2050 cm^{-1} with a maximum at around 2064 cm^{-1} and a weak absorption between 2050 and 2020 cm^{-1} (Fig. 2). After 2 ms the spectrum changes, showing major and minor bleaching maxima at 2064 and 2040 cm^{-1} respectively. The spectrum, which remains essentially unchanged for a period of at least 1 s, differs strikingly from that of the ground state, indicating a permanent photoproduct with an absorption maximum around 2052 cm^{-1}. The kinetics in the bleaching and absorption areas follow essentially a first-order law at lower intensity (5 and 6 in Fig. 3), the rate constant is $k \approx 2.5 \times 10^3\ s^{-1}$ and contains a second-order component at four times higher intensity (3 and 4 in Fig. 3). These observations reflect the existence of (i) an IR-absorbing stable photoproduct, *trans*-[Pt$(PPh_3)_2(N_3)_2$] [2,8], responsible for the permanent bleaching of the ground state sample, (ii) an IR-absorbing transient I_A ([$Pt^I(PPh_3)_2N_3$]), and (iii) a second photoproduct I_B, coordinatively unsaturated [$Pt^0(PPh_3)_2$], which does not absorb between 2100 and 2000 cm^{-1}:

$$cis\text{-}[Pt(PPh_3)_2(N_3)_2] \xrightarrow{h\nu} trans\text{-}[Pt(PPh_3)_2(N_3)_2] \quad (2)$$

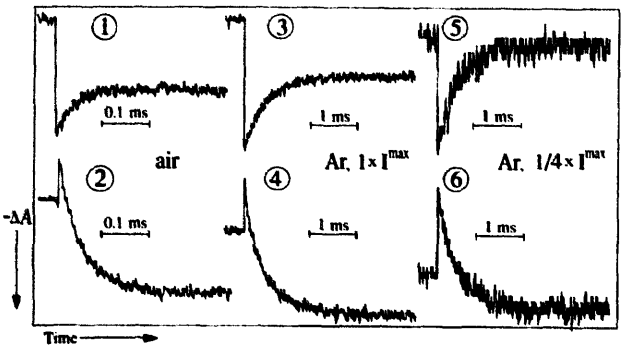

Fig. 3. Kinetics of *cis*-[Pt$(PPh_3)_2(N_3)_2$] in CH_2Cl_2 at 2052 cm^{-1} (upper traces) and 2040 cm^{-1} (lower traces); air-saturated (1,2) and Ar-saturated (3–6); note that the laser intensity in 5 and 6 is four times lower than in the other cases, $I^{max} \sim 8$ MW cm^{-2}.

$$cis\text{-}[Pt(PPh_3)_2(N_3)_2] \xrightarrow{h\nu} I_A([Pt^I(PPh_3)_2N_3]) \rightarrow I_B([Pt^0(PPh_3)_2]) \quad (3)$$

Similar spectral and kinetic results, e.g. $t_{1/2} \approx 0.3$ ms, were obtained in several solvents under Ar (Table 1). In air-saturated MeTHF, THF, $CHCl_3$, CH_2Cl_2 (1 and 2 in Fig. 3) and CH_3CN, both the decay of the initial transient and the formation of the second bleaching component are faster (Table 1). Thus, a value of $k_{ox} \approx 1.3 \times 10^7\ M^{-1}\ s^{-1}$ was estimated from the kinetics in Ar-, air- and O_2-saturated CH_2Cl_2 solutions. Furthermore, the reaction of I_A with O_2 leads again to a species that does not absorb in the 2080–2050 cm^{-1} range.

3.3. Steady-state IR absorption spectroscopy

In order to study the *cis* → *trans* photoisomerization and photodecomposition, the ground state IR absorption spectra were recorded after repeated flashing of *cis*-[Pt$(PPh_3)_2(N_3)_2$] in air- and Ar-saturated CH_3CN. Under both conditions, the shoulder at 2045 cm^{-1} disappears after 30–50% overall conversion, and the maximum is shifted from 2060 to ~2054 cm^{-1} (Fig. 2); eventually (>90% conversion) this IR absorption disappears completely owing to the loss of the two azide ligands. This shift would be consistent with Eqs. (2) and (3) with *trans*-[Pt$(PPh_3)_2(N_3)_2$] absorbing at 2052 cm^{-1}, and I_B being coordinatively unsaturated [$Pt^0(PPh_3)_2$] under Ar which does not absorb in this region. Similar experiments with [Pt(dppp)$(N_3)_2$] in Ar-saturated CH_2Cl_2, however, show a small shift of the maximum from 2060 to ~2057 cm^{-1} after 30–50% overall conversion (Fig. 1). A spectral shift rather than a complete disappearance of this IR band is surprising because of the fixed *cis* conformation of the complex. It might be due to Cl abstraction from the solvent or photoinduced generation of a di-μ-azido complex of the kind [(dppp)$Pt^0(N_3)_2Pt^{II}$(dppp)].

3.4. Time-resolved UV–Vis absorption spectroscopy

The transient UV–Vis absorption spectra of [Pt(dppp)$(N_3)_2$] and *cis*-[Pt$(PPh_3)_2(N_3)_2$] in Ar- and O_2-

saturated CH_2Cl_2 are shown on a short time-scale in Figs. 4 and 5. The spectra, which generally increase in ΔA during the 308 nm pulse, exhibit a maximum around 380 nm and a flank extending to ~550 nm. In several Ar-saturated solvents, e.g. MeTHF, THF, $CHCl_3$, CH_2Cl_2 and CH_3CN for *cis*-[$Pt(PPh_3)_2(N_3)_2$], the main effect is an increase in absorption in the 320–500 nm range after the laser pulse. Only a minor part of the increase in ΔA shows a time dependence (Figs. 4(a) and 5(a)), i.e. there is no simple correlation with the kinetics in the IR region. Subsequent formation of several intermediates with similar spectra mainly leads to the permanent changes (see below).

The behaviour is different in the presence of O_2, since only the initial increase in absorption in the 320–500 nm range is

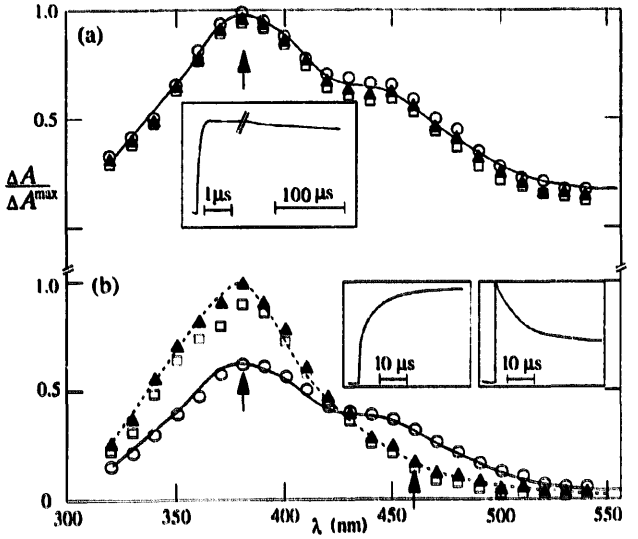

Fig. 4. Transient absorption UV–Vis spectra (ΔA^{max} ~0.2) of [$Pt(dppp)(N_3)_2$] in (a) Ar- and (b) O_2-saturated CH_2Cl_2 at 0.5 (○), 10 (▲) and 100 µs (□) after the pulse. Insets: kinetics at 380 nm (a) and 380 and 460 nm (b).

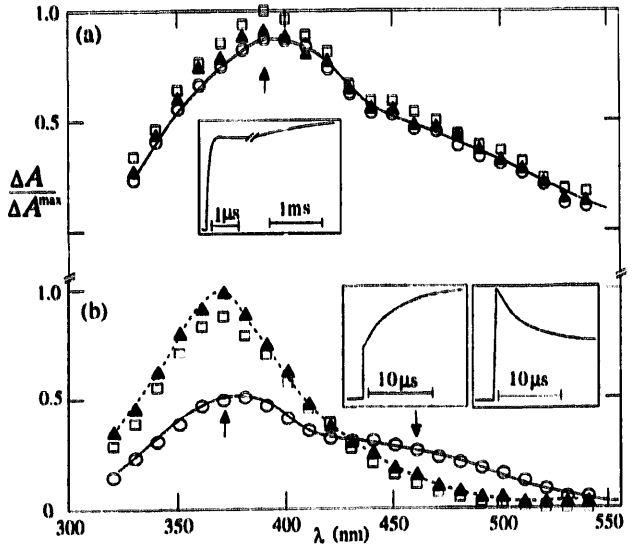

Fig. 5. Transient absorption UV–Vis spectra (ΔA^{max} ~0.2) of *cis*-[$Pt(PPh_3)_2(N_3)_2$] in (a) Ar- and (b) O_2-saturated CH_2Cl_2 at 0.5 (○), 10 (▲) and 100 µs (□) after the pulse. Insets: kinetics at 390 nm (a) and 370 and 460 nm (b).

Table 2
Lifetimes in the presence of O_2, obtained from UV–Vis measurements [a]

Compound	Solvent	τ (µs)	
		Air	O_2
[$Pt(dppp)(N_3)_2$]	$CHCl_3$	22	5
	CH_2Cl_2	42	8
	CH_3CN	36	
cis-[$Pt(PPh_3)_2(N_3)_2$]	MeTHF	15	2.8
	THF	25	4
	$CHCl_3$	25	4
	CH_2Cl_2	48	8
	CH_3CN	35	

[a] Decay observed at ~460 nm (same kinetics within experimental error were observed from the increase at ~380 nm); A_{308} = 0.2–0.6 (1 mm); the solutions were purged with air or O_2; in all cases the half-life under Ar is longer than 1 ms.

comparable with the spectrum in deoxygenated solution. Instead, after the pulse, ΔA in air- or O_2-saturated solution increases further in the 320–400 nm range, but decreases above 430 nm (Figs. 4(b) and 5(b)). The kinetics of formation of this second transient around 380 nm and decay at 450–500 nm are the same (or very similar) and depend both on the O_2 concentration and also marginally on the solvent. The spectral and kinetic changes for *cis*-[$Pt(PPh_3)_2(N_3)_2$] are in rough agreement with those reported before for air-saturated CH_3CN [6]. Moreover, the kinetics in the UV–Vis region are identical (within experimental error) with the decay of transient I_A ([$Pt^IP_2N_3$], $P_2 = (PPh_3)_2$ and dppp respectively, Table 2) in the IR. The rate constants for scavenging [$Pt^IP_2N_3$] by O_2 are $k_{ox} = (1.3–2.8) \times 10^7$ M^{-1} s^{-1}. From these results we conclude that (i) [$Pt^IP_2N_3$] is formed within 20 ns, (ii) [Pt^0P_2], formed subsequently, absorbs also in the UV, and (iii) [$Pt^IP_2N_3$] is scavenged by O_2.

After the initial photoreaction, a major part of the transient UV–Vis absorption spectrum of both complexes under Ar remains on a 1 ms to 1 s timescale. In the presence of O_2, however, only a minor part of ΔA is permanent, whereas the major part decays subsequently. This is illustrated in Fig. 6 for [$Pt(dppp)(N_3)_2$] in CH_2Cl_2.

Examples of the changes in ΔA_{380} on a 1 µs to 1 s timescale are shown in Fig. 7 for the two complexes in Ar- and O_2-saturated CH_2Cl_2. For [$Pt(dppp)(N_3)_2$] under Ar virtually no change could be detected and for *cis*-[$Pt(PPh_3)_2(N_3)_2$] only a slight increase was found within 1 ms followed by a permanent signal. This behaviour is strongly influenced by the presence of O_2, where ΔA_{380} decreases strongly between 0.3–10 ms. The pattern of the kinetics in Ar-, air- or O_2-saturated solution is somewhat solvent dependent, but in all cases the major part of the increase after the pulse remains permanent in the absence of O_2 and decays in its presence.

3.5. Steady-state UV–Vis absorption spectroscopy

Generally, upon repeated flashing at 308 nm of *cis*-[$Pt(PPh_3)_2(N_3)_2$] under Ar, the steady-state spectra

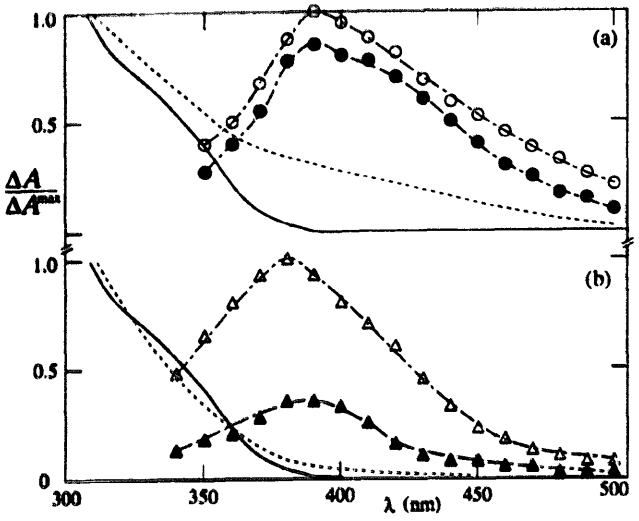

Fig. 6. Transient absorption UV–Vis spectra of [Pt(dppp)(N$_3$)$_2$] in (a) Ar- and (b) O$_2$-saturated CH$_2$Cl$_2$ at 0.2 ms (open symbols) and 20 ms (full symbols) after the pulse; ground state spectrum prior to and after ~30 pulses (full and dashed lines respectively).

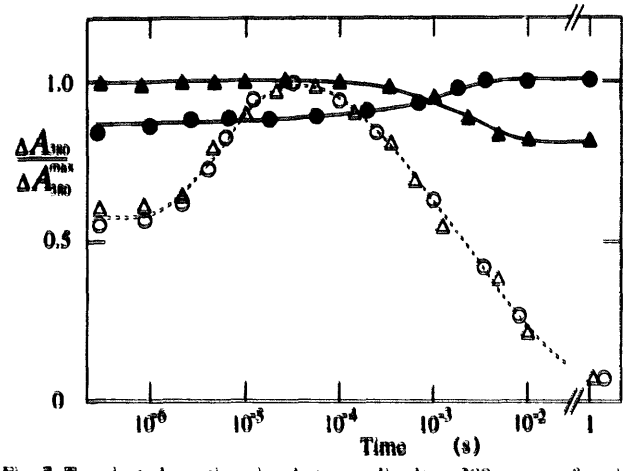

Fig. 7. Transient absorption signals (normalized) at 380 nm as a function of time (note log scale) for *cis*-[Pt(PPh$_3$)$_2$(N$_3$)$_2$] (circles) and [Pt(dppp)(N$_3$)$_2$] (triangles) in Ar- and O$_2$-saturated CH$_2$Cl$_2$ (full and open symbols respectively).

decrease below 300 nm and increase above 330 nm. This is due to photodecomposition and formation of the dimer, [Pt$_2$(PPh$_3$)$_4$], respectively [6–9]. The increase in absorption at $\lambda > 330$ nm is much smaller in O$_2$- or air-saturated than Ar-saturated solution; in particular, isosbestic points were found under air at 321, 326 and 319 nm in THF, CHCl$_3$ and CH$_3$CN respectively. Photodecomposition was also observed for [Pt(dppp)(N$_3$)$_2$] in several solvents. The absorption spectra of [Pt(dppp)(N$_3$)$_2$] in Ar- and O$_2$-saturated CH$_2$Cl$_2$ are shown in Fig. 6(a) and (b) respectively. They are similar to those of *cis*-[Pt(PPh$_3$)$_2$(N$_3$)$_2$]. The quantum yields of the disappearance of *cis*-[Pt(PPh$_3$)$_2$(N$_3$)$_2$] in Ar-saturated CH$_2$Cl$_2$ are $\Phi = 0.07$, 0.10 and 0.095 for irradiation wavelengths of 254, 313 and 366 nm respectively [9]. Similar Φ values (0.07–0.10) under these irradiation conditions have been obtained in THF and ethanol [15]; i.e. different transitions in the complex as well as solvents of medium and strong polarity have only a small effect on Φ.

3.6. Discussion

The two compounds under examination are representative examples of mixed-ligand platinum(II) azido complexes which differ by their coordination of monophosphine and diphosphine ligands. The intense IR absorption of these complexes in the 2100–2000 cm^{-1} range, attributed to the stretching frequencies of the azide ligands [8,11], render the dynamics of the two primary photoprocesses of *cis*-[Pt(PPh$_3$)$_2$(N$_3$)$_2$], photoisomerization and intramolecular electron transfer, accessible to IR monitoring.

Since [Pt(dppp)(N$_3$)$_2$] cannot photoisomerize (Scheme 1), electron transfer with formation of [Pt^{I}(dppp)N$_3$] as the transient I_A and [Pt^{0}(dppp)] as the product I_B are the obvious alternatives (P_2 = dppp, Figs. 1 and 8):

$$[Pt^{II}P_2(N_3)_2] \xrightarrow{h\nu} [Pt^{I}P_2N_3] + {}^{\cdot}N_3 \quad (4)$$

$$[Pt^{I}P_2N_3] \rightarrow [Pt^{0}P_2] + {}^{\cdot}N_3 \quad (5)$$

$$2\,{}^{\cdot}N_3 \rightarrow 3N_2 \quad (6)$$

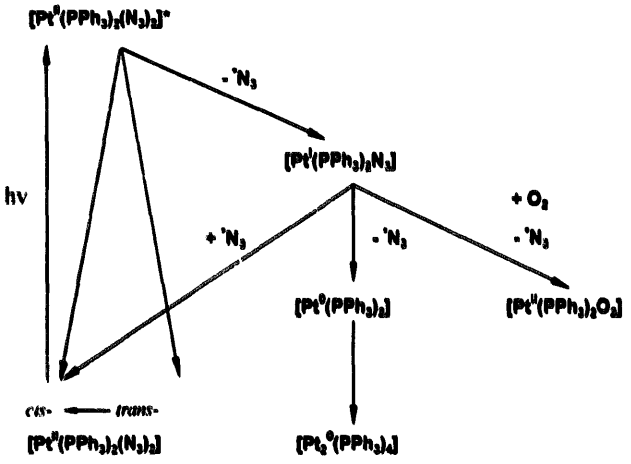

Scheme 1.

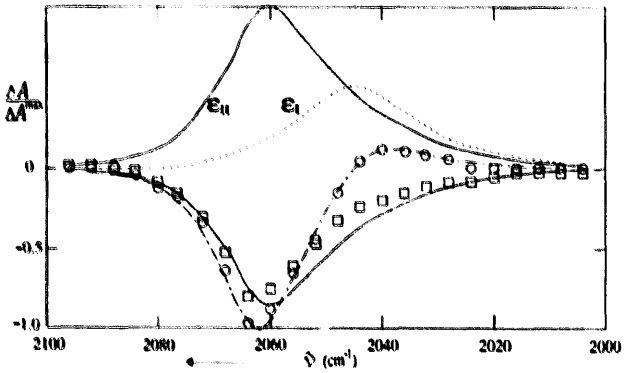

Fig. 8. Calculated transient difference spectrum of [Pt(dppp)(N$_3$)$_2$] in Ar-saturated CH$_2$Cl$_2$ at the end of the 308 nm pulse (— · —) assuming the absorption spectrum of [Pt^{I}(dppp)N$_3$] (- - -); the full line refers to the ground state of [Pt(dppp)(N$_3$)$_2$].

The observation of the generation of azidyl radicals and platinum(I) complex fragments in the primary photoprocess of $[Pt^{II}(PPh_3)_2(N_3)_2]$ by means of ESR spin trapping [6] and UV–Vis flash photolysis [7], as well as low-temperature luminescence [9] and steady-state IR absorption spectroscopy [8], have already been reported. The azidyl radical absorbs in the UV, $\lambda_{max} = 274$ nm, $\varepsilon_{274} = 2.0 \times 10^3$ M^{-1} cm^{-1}, and the rate constant $2k_6$ is known from pulse radiolysis to be 9×10^9 M^{-1} s^{-1} in aqueous solution [16]. In order to account for the intensity dependence of the bleaching recovery kinetics, Eq. (7) is considered:

$$[Pt^{I}P_2N_3] + {}^{\cdot}N_3 \rightarrow [Pt^{II}P_2(N_3)_2] \quad (7)$$

Another reaction of the azidyl radicals is unlikely under our conditions. Recently, the addition of azidyl radicals to olefins in CH_3CN yielding transients with absorption maxima around 2000 cm^{-1} has been reported [17].

Electron transfer via Eqs. (4) and (5) and involvement of Eq. (7) in the case of $[Pt(dppp)(N_3)_2]$ is also supported by the following. The laser-induced spectral changes are due to $\Delta A/l = \{\varepsilon_I \text{conc.}(1)_t - \varepsilon_{II}\Delta\text{conc.}(2)_t\}$, where conc.(1)$_t$ is the concentration of $[Pt^{I}(dppp)N_3]$ at the time $t = 3$ μs or 2 ms and conc.(2)$_t$ the corresponding concentration of $[Pt^{II}(dppp)(N_3)_2]$, i.e. the values are conc.(1)$_t$ = conc.(2)$_t$ at $t = 3$ μs. The observed spectrum (circles in Fig. 8) can be composed by using ε_I ($\lambda_{max} = 2045$ cm^{-1}, dotted line) and ε_{II} (full line). The reduced bleaching after 2 ms (squares in Fig. 8) in the 2080–2060 cm^{-1} range is due most probably to a decrease in Δconc.(2)$_t$, i.e. due to Eq. (7). Since the spectrum after 2 ms is not fully that which one expects from photodecomposition alone (Fig. 8) and because of the shift of the steady-state IR band (Fig. 1), halogen abstraction from the solvent yielding $[Pt^{II}(dppp)N_3Cl]$, dimerization of $[Pt^{I}(dppp)N_3]$ or a so-far unknown photoinduced reaction of $[Pt^{0}(dppp)]$ and $[Pt^{II}(dppp)(N_3)_2]$ to $[(dppp)Pt^{II}(N_3)_2Pt^{II}(dppp)]$ may be considered and remains to be elucidated experimentally.

The eventual steps of the coordinatively unsaturated platinum(0) complexes leading to the stable product(s) in the absence of O_2 (Scheme 1) have been proposed to be a reaction with the solvents S, Eq. (8), and dimerization, Eq. (9) [1,7,8]:

$$[Pt^{0}P_2] + 2S \rightarrow [Pt^{0}P_2S_2] \quad (8)$$

$$2[Pt^{0}P_2S_2] \rightarrow [Pt^{0}_2(P_2)_2] + 4S \quad (9)$$

Platinum(0) complex fragments have been detected by luminescence spectroscopy at low temperatures [9,18,19]. The role of the solvent in Eqs. (8) and (9) has been discussed previously [1,7,8]. By time-resolved UV–Vis studies of *cis*-$[Pt^{II}(PPh_3)_2(N_3)_2]$ and $[Pt^{II}(dppp)(N_3)_2]$, we could not observe any significant changes in the time range of 1 ms to 1 s in several solvents under Ar (Figs. 4(a), 5(a), 6(a) and 7). Other methods are required to investigate the eventual reaction processes.

For *cis*-$[Pt(PPh_3)_2(N_3)_2]$, *cis* → *trans* photoisomerization, Eq. (2), has to be postulated to account for the time-resolved IR spectra (Figs. 3 and 9). In addition Eqs. (4) and (5) are suggested. The assignment of the initial transient to $[Pt^{I}(PPh_3)_2N_3]$ is supported by the findings that transient I_X is formed within 2–3 μs and decays with $t_{1/2} \approx 0.3$ ms and that the IR spectrum is virtually the same as that obtained from $[Pt(dppp)(N_3)_2]$ (Figs. 1 and 2). Note that small differences between the spectra of the initial transients, $[Pt^{I}P_2N_3]$, are due to the fact that in the case P = PPh_3 a certain amount of the *cis* isomer is photoconverted into the *trans* isomer which may slowly isomerize back.

The decrease in bleaching in the 2080–2060 cm^{-1} range for *cis*-$[Pt(PPh_3)_2(N_3)_2]$ between 3 μs and 2 ms (Fig. 9, circles and squares respectively) is attributed to an increase in the concentration of $[Pt^{II}(PPh_3)_2(N_3)_2]$ (*cis* and possibly *trans* isomer), i.e. Eq. (7). The spectral changes are due to $\Delta A/l = \{\varepsilon_I \text{conc.}(1)_t + \varepsilon_I \text{conc.}(trans)_t - \varepsilon_{II}\Delta\text{conc.}(cis)_t\}$, where conc.(1)$_t$, conc.(*trans*)$_t$ and conc.(*cis*)$_t$ are the concentrations of $[Pt^{I}(PPh_3)_2N_3]$, *trans*-$[Pt^{II}(PPh_3)_2(N_3)_2]$ and *cis*-$[Pt^{II}(PPh_3)_2(N_3)_2]$ at appropriate times respectively, and $\Delta\text{conc.}(cis)_t = \text{conc.}(1)_t + \text{conc.}(trans)_t$. The observed spectrum at $t = 2$ ms (where conc.(1)$_t$ is zero) can be composed by those using ε_I ($\lambda_{max} = 2044$ cm^{-1}, dashed line) and ε_{II} (full line). The changes at $t = 3$ μs can be calculated from the spectra in Fig. 9 ($\lambda_{max} = 2050$ cm^{-1} for ε_I, dotted curve) by using the term $\varepsilon_I + \varepsilon_I - \alpha\varepsilon_{II}$, where the constant $\alpha = 1.4$ refers to the finding that the amount of bleaching, $\Delta\text{conc.}(cis)_t$, is reduced between 3 μs and 2 ms. Here, we assume that Eq. (7) leads to the *cis* rather than the *trans* isomer, i.e. conc.(*trans*)$_t$ is independent of t.

To account for the scavenging of intermediate I_X by O_2 (Tables 1 and 2) and the further effects caused by O_2 (Figs. 4(b), 5(b), 6(b) and 7), we propose Eq. (10) [1,7]:

$$[Pt^{I}P_2N_3] + O_2 \rightarrow [Pt^{II}P_2O_2] + {}^{\cdot}N_3 \quad (10)$$

$$[Pt^{0}P_2] + O_2 \rightarrow [Pt^{II}P_2O_2] \quad (11)$$

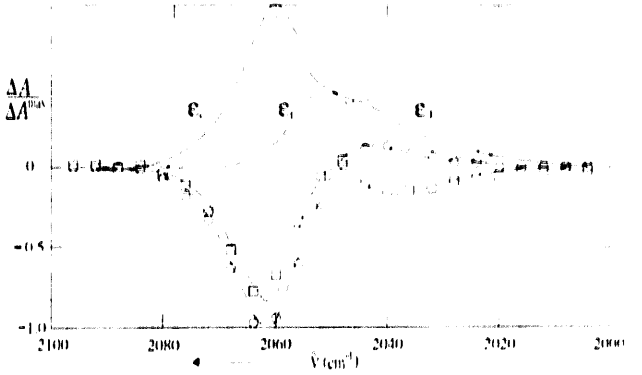

Fig. 9. Calculated transient difference spectra of *cis*-$[Pt(PPh_3)_2(N_3)_2]$ in Ar-saturated CH_2Cl_2 at the end of the 308 nm pulse (– – –) and after reaching the stationary mixture (— · · —) using the absorption spectra of *cis*-$[Pt(PPh_3)_2(N_3)_2]$ (ε_{II} line), *trans*-$[Pt(PPh_3)_2(N_3)_2]$ (ε_I line) and $[Pt^{I}(PPh_3)_2N_3]$ (ε_I line).

Generally, the differences in the steady-state UV–Vis absorption spectra in the absence and presence of O_2 may be due to Eqs. (8)/(9) and Eqs. (10)/(11) respectively.

4. Conclusions

The primary photoreduction of *cis*-diazido-bis(triphenylphosphine)platinum(II) (*cis*-[$Pt^{II}(PPh_3)_2(N_3)_2$]) competes with the isomerization to *trans*-[$Pt^{II}(PPh_3)_2(N_3)_2$]. *Trans*-[$Pt^{II}(PPh_3)_2(N_3)_2$] itself is reduced photochemically to the same intermediates, namely monoazido-bis(triphenylphosphine)platinum(I) and the azidyl radical. Subsequent dark reactions yield the coordinately unsaturated [$Pt^0(PPh_3)_2$] complex fragment and [$Pt_2(PPh_3)_4$] as stable product as summarized in Scheme 1. The primary photoreaction of diazido-1,3-bis(diphenylphosphino)propaneplatinum(II) ([$Pt^{II}(dppp)(N_3)_2$]) leads to the azidyl radical and the corresponding platinum(I) intermediate which decays subsequently in several steps to [$Pt_2(dppp)_2$]. The platinum(I)/(0) intermediates of both complexes are efficiently scavenged by oxygen.

Acknowledgements

We thank Dr W. Klotzbücher for his support and Messrs D. Pagirnus, G. Klihm, C. Berling, Mr K.-H. Toepfer, J. Sehnert and L.J. Currell for technical assistance. The work in Leipzig was supported by the Fonds der Chemischen Industrie and the Deutsche Forschungsgemeinschaft (DFG). A.K.C. acknowledges also a personal fund by the DFG.

References

[1] H. Hennig, R. Stich, H. Knoll, D. Rehorek and D.J. Stufkens, Coord. Chem. Rev., 111 (1991) 131.
[2] C. Bartocci and F. Scandola, Chem. Commun., (1970) 531.
[3] R. Ngai, F. Wang and J.L. Reed, Inorg. Chem., 24 (1985) 3803.
[4] H. Hennig, K. Hofbauer, K. Handke and R. Stich, Angew. Chem., 109 (1997) 373; Angew. Chem., Int. Ed. Engl., 36 (1997) 408.
[5] K.S. Suslick, F.V. Acholla and B.R. Cook, J. Am. Chem. Soc., 109 (1987) 2818.
[6] H. Hennig, R. Stich, D. Rehorek, P. Thomas and T.J. Kemp, Inorg. Chim. Acta, 143 (1988) 7.
[7] H. Hennig, R. Stich, H. Knoll and D. Rehorek, Z. Anorg. Allg. Chem., 576 (1989) 139.
[8] H. Knoll, R. Stich, H. Hennig and D.J. Stufkens, Inorg. Chim. Acta, 178 (1990) 71.
[9] H. Hennig, K. Ritter, H. Knoll and A. Vogler, Inorg. Chim. Acta, 211 (1993) 117.
[10] J.L. Reed, Y.-H.L. Wang and F. Basolo, J. Am. Chem. Soc., 94 (1972) 7173.
[11] C.-J. Oetker and W. Beck, Spectrochim. Acta A, 29 (1973) 1975.
[12] W. Beck, W.P. Fehlhammer, P. Pöllmann, E. Schuierer and K. Feldl, Chem. Ber., 100 (1967) 2335.
[13] K. Schaffner and F.-W. Grevels, J. Mol. Struct., 173 (1988) 51.
[14] H. Görner, Photochem. Photobiol., 52 (1990) 935.
[15] K. Ritter, Diplomarbeit, Universität Leipzig, 1992.
[16] Z.B. Alfassi and R.H. Schuler, J. Phys. Chem., 89 (1985) 3359.
[17] M.S. Workentin, B.D. Wagner, J. Lusztyk and D.M. Wayner, J. Am. Chem. Soc., 117 (1995) 119.
[18] A. Vogler, R.E. Wright and H. Kunkely, Angew. Chem., 92 (1980) 745.
[19] S. Oishi and K. Suzuki, Chem. Lett., (1991) 171.